

## Variability in Large-Scale Water Balance with Land Surface–Atmosphere Interaction

DARA ENTEKHABI, IGNACIO RODRIGUEZ-ITURBE,\* AND RAFAEL L. BRAS

Ralph M. Parsons Laboratory, Department of Civil Engineering, Massachusetts Institute of Technology, Cambridge, Massachusetts

(Manuscript received 3 April 1991, in final form 22 November 1991)

### ABSTRACT

Persistent and prolonged periods of dry or moist conditions are often evident in the interannual variability of continental-type climates. This variability appears as fluctuations around several distinct and preferred moisture states. These fluctuations and transitions between the preferred states are commonly attributed to large-scale changes in atmospheric circulation patterns possibly caused by oceanic influence.

This paper argues that a major contributing factor to the persistent dry or moist behavior could be due to feedback and nonlinear interaction between the components of the hydrologic cycle in both the land and the atmosphere. A model that couples the water balance of continental landmasses and the overlying atmosphere is presented. The large-scale variabilities in atmospheric circulation are introduced by way of simple randomness in key forcing parameters. The result is a multiplicative-noise stochastic differential equation for the water balance dynamics of continental-type climates that includes land surface–atmosphere interaction.

The solution to this differential equation exhibits a bimodal probability distribution function for soil moisture and precipitation. Extended periods of anomalous dry conditions (drought) or alternatively wet conditions (pluvial), with abrupt transitions between them, are present in the model. The statistics of persistent anomalous conditions are analyzed for two climatic classifications. The probability distribution function for transitions out of droughts are developed for the modeled climates.

### 1. Introduction

An important problem in hydroclimatology and one that often has devastating consequences for human systems is the interannual persistence of dry anomalies or droughts. Figure 1 illustrates the variability in the annual rainfall of several sub-Saharan regions. The normalized time series exhibit multiyear periods of dry or moist anomalies with abrupt transitions between them. The drought periods in the early part and the end of the record persist for several years and up to over a decade.

The prediction of the onset and estimates of the duration of droughts has received widespread attention. Numerous meteorological conditions that lead to the initiation of droughts and many feedback mechanisms that are responsible for the prolonged duration of these anomalies have been identified for various regions over the globe. The voluminous literature that has emerged from these analyses does not, and for obvious reasons cannot, lead to a general theory of why droughts occur and how their dynamics evolve in time. With respect

to droughts, Namias (1983) writes: “as with many meteorological and climatological phenomena, there is never only one, but multiple causes.” Furthermore, it is plausible that a particular region may experience recurring droughts that are brought about by different preconditions and persist for different reasons. The analyses of many historical droughts, either by the statistical analyses of observed data or by conditional simulation with numerical models, nevertheless provide at least a descriptive understanding of some general features of this important hydroclimatological phenomenon.

The initiation of droughts over large continental regions is generally related to anomalous features in the general circulation of the atmosphere. The exact nature of these teleconnective disturbances and the reasons for their development are dependent on the specifics of the situation. Large-scale heating anomalies associated with shifts in seasonal sea surface temperature (SST) patterns are often identified as the forcing factor for the development of general circulation features that initiate droughts over large continental regions [see Voice and Hunt (1984) for a review]. Displaced jet streams and the advection and blocking of anticyclonic vorticity over the continents then leads to subsiding air that warms adiabatically and lowers the relative humidity (Namias 1983). In the tropics, the intertropical convergence zone (ITCZ) may experience shifts in position or changes in intensity due to the anomalous SST forcing (Nicholson and Entekhabi 1986). This in

\* Also affiliated with Instituto Internacional de Estudios Avanzados, Caracas, Venezuela.

Corresponding author address: Dr. Dara Entekhabi, Massachusetts Institute of Technology, Department of Civil Engineering, Ralph Parsons Laboratory, 48–331, Cambridge, MA 02139.

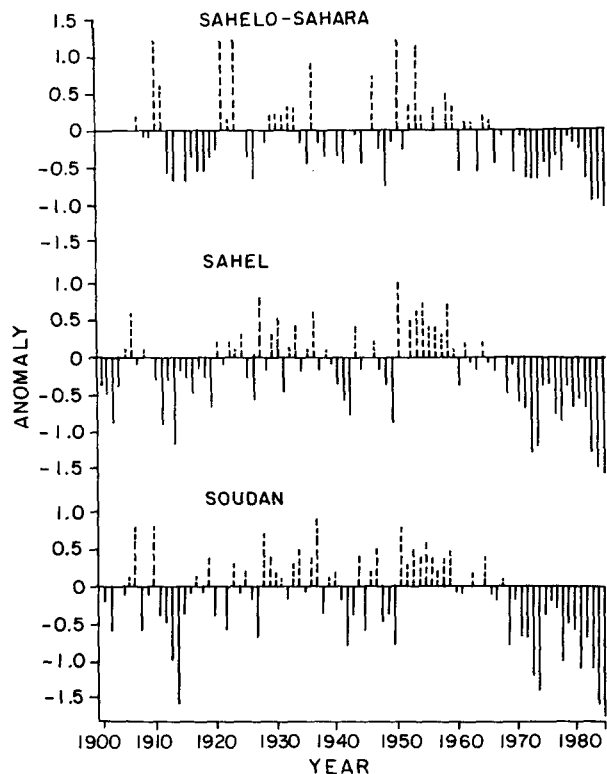


FIG. 1. Standardized time series of annual rainfall in sub-Saharan Africa (from Nicholson and Entekhabi 1986).

turn will affect the precipitation and latent heating in the tropic and subtropic atmosphere.

Due to the multiplicity of conditions that may lead to drought, an anomalous general circulation feature may be a necessary condition, but it is not a sufficient condition for the development of a severe and sustained drought. The development and growth of feedback mechanisms are what transform an anomalous perturbation into a persistent and prolonged drought. In fact, it is the identification and understanding of these feedbacks that is the main challenge in the scientific analysis of droughts.

In semiarid regions for example, the vegetation cover may be reduced in response to an anomalous precipitation deficit; the reduced vegetation cover results in a higher surface albedo. The land surface may then lose more radiative energy to space than it gains from absorbed solar radiation. The local region thus becomes a net sink of energy with respect to the global energy balance, and the overlying atmosphere develops into a state that favors the further inhibition of precipitation. Despite the net energy loss, the air itself is warmed due to the strong subsidence and adiabatic heating. This feedback mechanism is referred to as the Charney biogeophysical hypothesis, and variations of it have strongly influenced the treatment of drought phenomena in the literature (Charney et al. 1977). Similar

surface feedbacks may develop due to the drying of the surface soil and the associated rise in its albedo (Idso et al. 1975). Anthropogenic damage to the vegetation and topsoil may also reinforce the drought. This may lead to the more devastating desertification, which refers not only to a loss of biological productivity but also to a degradation of the microclimate (Hare 1985). The reduction in the vegetation cover also leads to a lowered surface roughness and thus reduced land surface-atmosphere exchange of momentum, mass, and heat. There have been several suggestions but no established evidence that this is a contributing factor to the prolonged duration of drought conditions. The loss of the vegetation cover and the drying of the surface soil results in the enhanced generation of dust. These small airborne particles act as nuclei for the formation of small liquid droplets in the atmosphere. During droughts, the abundance of smaller droplets inhibits coalescence, which is needed for the efficient formation of larger raindrops (Namias 1983). The relative deficiency of larger droplets, droplets that have sufficient terminal velocities to reach the surface as precipitation and can survive evaporation in their descent, reinforces the drought conditions by further reducing the precipitation.

Figure 2 [originally from Chagnon (1987)] illustrates the propagation of perturbations in precipitation through the land branch of the hydrologic cycle. When a precipitation anomaly due to factors that initiate

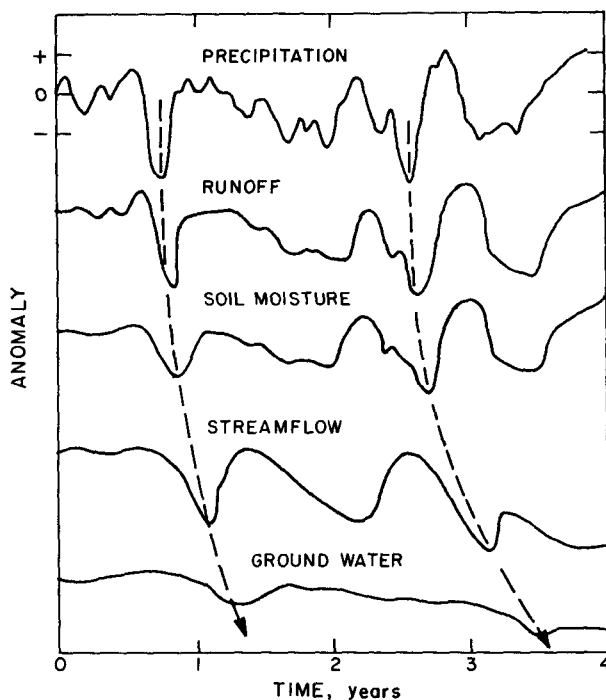


FIG. 2. The propagation of a perturbation in precipitation amount through the land branch of the hydrologic cycle [after Chagnon (1987) in McNab (1989)].

droughts occurs (e.g., a general circulation anomaly or teleconnection), the surface runoff and soil moisture are reduced. The contribution to stream flow and groundwater recharge are in turn diminished. Since the anomaly propagates through components of the hydrologic cycle with successively longer memory (follow the dashed line from top to bottom in Fig. 2), the effects of the original perturbation in precipitation are hence prolonged in time.

One important factor not explicitly illustrated in Fig. 2 is the possible propagation of anomalies in the reverse direction. What if there are ways in which the anomalies that propagated from the top (precipitation), and successively marched through the components of the hydrologic cycle with longer and longer memory, had a route back and would feedback on the precipitation through moisture supply? The consequences would clearly be prolonged droughts, since the forcing would now be originating from sources with long memory.

Soil moisture control of large-scale and long-term surface heat and moisture balance are important feedback mechanisms that often contribute to the persistence of dry conditions (Yeh et al. 1984; Rowntree and Bolton 1983; Stidd 1975). The reduced surface soil moisture, through radiative, thermodynamic, and moisture-supply processes, leads to the conditions that favor continued drought. The soil moisture reservoir has memory considerably longer than that of most atmospheric processes. Thus, an anomalous perturbation may persist through processes dependent on soil moisture.

The sequence of events in Fig. 2 are clearly a part of most severe droughts. Such a scenario and the potential feedback of moisture stored in surface and subsurface reservoirs on the supply of precipitation have received widespread consideration (Eltahir 1989; Koster et al. 1986; Lettau et al. 1979; Budyko 1974; Stidd 1975; McDonald 1962). In addition to all the potential feedback mechanisms identified for droughts in the preceding paragraphs, we consider this soil moisture supply mechanism, especially for continental climates that derive a large portion of their precipitation from local (e.g., continental soil water storage) rather than advected evaporative sources, to be an important factor in explaining the influence of surface hydrologic processes on the observed persistence of drought. Using aerological observations of water vapor flux, Brubaker et al. (1991) give quantitative estimates of the fraction of locally derived precipitation for various continental regions in North and South America, Asia, and Africa.

The strong influence of land surface-atmosphere interaction in prolonging anomalous dry conditions is evident in the observation that innercontinental regions tend to be more drought prone and that droughts persist longer in the interior land regions (Diaz 1983; Karl 1983). Karl et al. (1987) demonstrate that once drought is initiated, the probability of transition out of the anomalous state is less for the interior portions

of the continent where precipitation recycling, as estimated by Brubaker et al. (1991), is strongest.

In this paper, we present a set of coupled water balance equations for the soil storage and the atmospheric air column overlying large continental regions (Rodriguez-Iturbe et al. 1991). The influence of general circulation or teleconnective factors that initiate droughts is modeled as simple white noise random perturbations in key forcing parameters. The result is a stochastic differential equation (SDE) for the water balance of large continental regions. The hydrologic components (runoff and evapotranspiration) for this model are physically based as nonlinear functions of the state of the surface soil moisture.

This simple model of the hydroclimatology of large continental regions exhibits persistent drought (and pluvial) anomalies. The stochastic perturbations, an analogy for year-to-year random variations in large-scale atmospheric flow features, occasionally trigger a fluctuation-induced transition to drought conditions that persist due to the nonlinear influences imbedded in the model.

The occurrence and duration of these droughts in the SDE model of continental water balance are analyzed in this paper. The statistical distribution of drought durations for two climatic case examples are developed. Through this simple model of the hydroclimatology of continental-type climates, we illustrate the importance of hydrologic land surface-atmosphere interaction in the dynamics of regional climate.

## 2. The water balance equation: Stochastic formulation

### a. Hydrologic fluxes

The surface hydrologic balance for a large-scale continental region is represented by the changes in the areal-mean soil moisture (Rodriguez-Iturbe et al. 1991):

$$nZ_r \frac{ds}{dt} = P(s) - Q(s) - E(s), \quad (1)$$

where  $nZ_r$  is the product of the soil porosity and the hydrologically active soil depth. The state variable  $s$  is the saturated fraction of this total depth that is available for moisture storage; that is, it is the relative soil saturation  $0 \leq s \leq 1$ . The differential change in storage depth  $nZ_r$  is equal to the difference between precipitation rate  $P(s)$  and the runoff and evapotranspiration losses  $Q(s)$  and  $E(s)$ .

The runoff and the actual evapotranspiration rates depend on the surface moisture condition as symbolized by the argument  $s$  in the functional form of these processes in Eq. (1). As empirical but physically consistent parameterizations,

$$\frac{Q(s)}{P(s)} = \epsilon s^r \quad (2)$$

and

$$\frac{E(s)}{E_p} = s^c \quad (3)$$

are given, where  $\epsilon$ ,  $r$ , and  $c$  are nonnegative constants. Equation (2) represents the runoff ratio or the fraction of precipitation that is direct runoff. It is empirically related to the relative soil saturation by a power law; little runoff is generated when the soil is dry ( $s \rightarrow 0$ ), and greater runoff is generated for humid conditions ( $s \rightarrow 1$ ). The runoff ratio is also confined to the interval  $[0, 1]$ , and it can be nonlinearly related to soil moisture depending on the parameter  $r$ .

The evapotranspiration rate is also proportional to the relative soil saturation in a nonlinear manner (linear if  $c = 1$ ). The maximum evaporation rate is confined to be less than or equal to the potential evaporation  $E_p$  rate, which is the evaporation rate if the water is nowhere limiting, and the loss rate is restricted by the available energy at the surface. The parameter  $c$  depends on soil and vegetation characteristics; Fig. 3 gives an overview of some evaporation efficiency estimates that are analogous to Eq. (3).

*b. Atmospheric feedback*

In the balance Eq. (1), the precipitation input itself is conceptualized to be functionally related to the governing soil moisture. The land surface-atmosphere interaction is intended to be represented through this functional dependence.

The precipitation water over large continental regions is derived from the advected (lateral and vertical) moisture in the overlying atmosphere, as illustrated in Fig. 4. By developing a water balance for the overlying

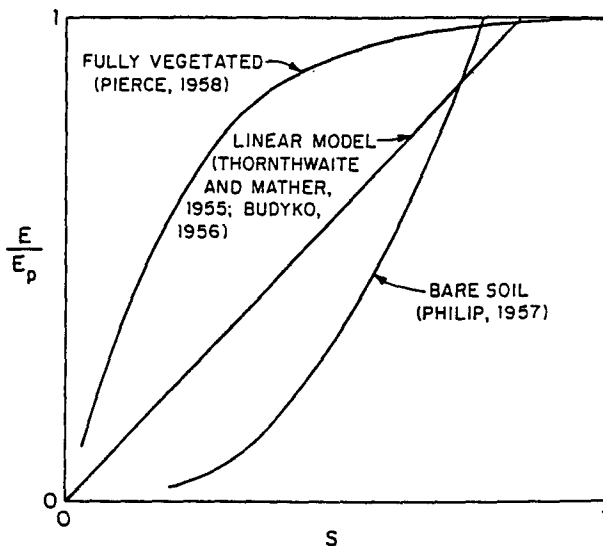


FIG. 3. The evaporation rate, normalized by its climatic potential value, as a function of relative soil saturation and for different surface types [after Lowry (1959) in Eagleson (1982)].

atmospheric moisture reservoir and coupling it to the balance for the surface reservoir in Eq. (1), a model is constructed for the surface and atmospheric interaction in the overall moisture supply for large continental regions.

The water vapor balance for the overlying atmosphere is performed by separating the precipitation into that derived from outside of the region (through lateral advection),  $P_a$ , and that derived from local evaporative sources,  $P_m(s)$ . The total precipitation is

$$P(s) = P_a + P_m(s). \quad (4)$$

The supply of precipitation water by the advection of moisture from outside of the region is independent of the hydrologic conditions over the continent. The local source of precipitation contributing to the amount  $P_m(s)$  of the total is, however, related to the surface evapotranspiration over the continent itself. Through this latter moisture supply mechanism, the total precipitation rate is functionally related to the governing areal-average soil moisture  $s$ , that is,  $P(s)$ . Next a physically based parameterization, based on the Budyko (1974) concept, will be derived for this functional form.

The supply of moisture laterally advected to the region is the product  $wu$ . Here  $w$  is the vertically integrated water vapor (precipitable) depth in the upwind source region

$$w = \frac{1}{\rho_L g} \int_{p_s}^0 q(p) dp. \quad (5)$$

That is, precipitable depth  $w$  is the vertical integral of specific humidity  $q(p)$  from the surface ( $p_s$ ) to an elevation in the atmosphere where pressure  $p$  vanishes. Here  $\rho_L$  and  $g$  are the liquid water density and gravitational acceleration of the earth. Thus  $w$  is in units of volume of water per unit area or simply depth;  $w$  is on the order of 0.01–0.04 m. The  $u$  term in the lateral incoming moisture supply rate  $wu$  is a weighted average of the wind vector normal to the boundaries of the region. The wind speed is weighted according to the specific humidity profile,

$$u = \frac{\int_{p_s}^0 u(p) q(p) dp}{\int_{p_s}^0 q(p) dp}. \quad (6)$$

Hence  $wu$  represents the rate of incoming supply of moisture from sources outside of the continental region. As evident in Eq. (4), an amount  $P_a$  of this total supply rate is removed from the atmospheric reservoir over the continent and precipitated onto the land surface. Hence, of the incoming rate  $wu$ , only the rate  $wu - P_a$  leaves the territory.

The other remaining source of precipitation water is the continent itself. There is moisture input into the

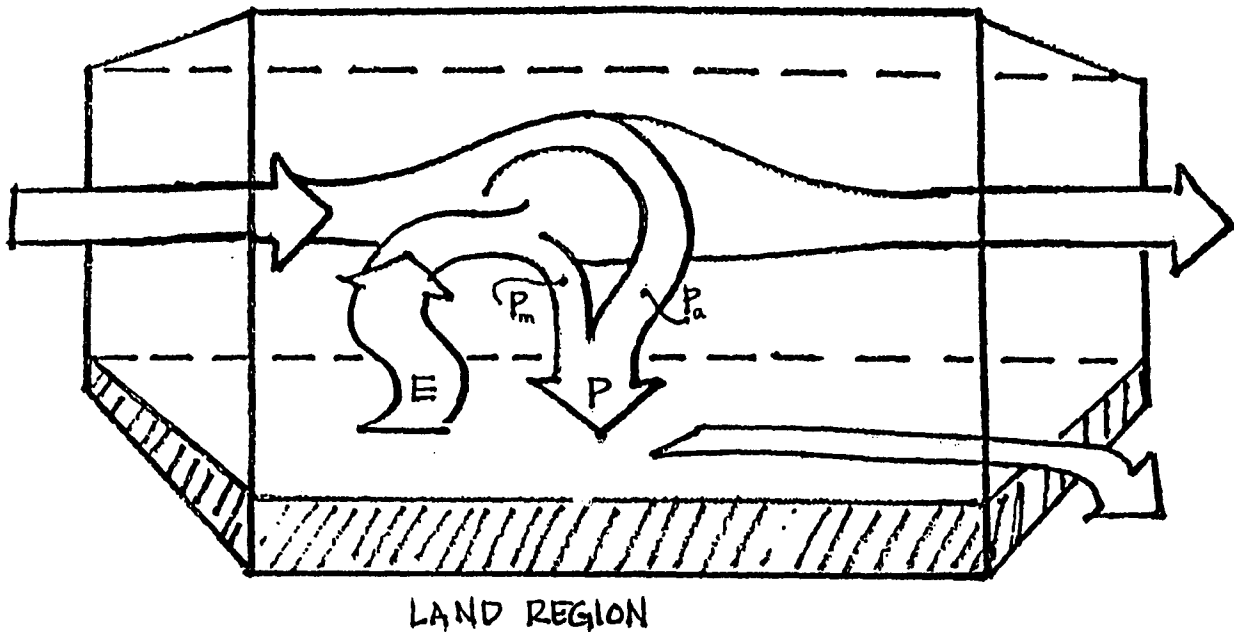


FIG. 4. The advective and local components of moisture supply to the total precipitation over large land areas (from Brubaker et al. 1991).

atmospheric reservoir from its bottom boundary as the flow traverses over the territory. Along a streamline and at distance  $v$  from the boundary (where the air mass streamtube intersects the region border), the cumulative of the evapotranspiration input  $E(s, v')$  is

$$\int_0^v E(s, v') dv'. \quad (7)$$

When an areal-average is taken along a streamline of length  $L$ , then the total input of the moisture derived from local sources into the atmospheric reservoir is  $E(s)L$ . And after substituting Eq. (3),  $E_p s^c L$ . Although there is no lateral inflow from this source, there is a lateral outflow  $(E_p s^c - P_m(s))L$ , representing the local supply minus the amount that is precipitated within the region.

A linear average of the lateral input and output of moisture at the two ends where the atmospheric air mass streamtube intersects the territorial boundaries is made. The average flux of externally derived moisture over the region is found to be

$$\frac{wu + (wu - P_a L)}{2} = wu - \frac{1}{2} P_a L. \quad (8)$$

The average flux of locally derived moisture over the atmosphere of the territory and along the same streamline is

$$\frac{0 + (E_p s^c - P_m(s))L}{2} = \frac{1}{2} (E_p s^c - P_m(s))L. \quad (9)$$

Assuming that the moisture derived from the external and local sources mix effectively over the territory, then ratio of precipitation derived from each source ( $P_m(s)/P_a$ ) equals to the ratio of the average flux rates in the overlying air mass. From Eqs. (8) and (9), expressions for these average rates for each source are given as

$$\frac{P_m(s)}{P_a} = \frac{\frac{1}{2} (E_p s^c - P_m(s))L}{wu - \frac{1}{2} P_a L}. \quad (10)$$

Now substitute Eq. (10) into Eq. (4) to find total precipitation and to determine its dependence on the continental soil moisture conditions:

$$P = P_a \left[ 1 + \frac{P_m(s)}{P_a} \right] = P_a \left[ 1 + \frac{s^c}{\Omega} \right], \quad (11)$$

where the nondimensional climatic parameter  $\Omega = LE_p/2wu$  has been defined. The parameter  $\Omega$ , containing the wind, streamtube characteristics, and parameters of the larger-scale forcing of the regional climate, is regarded to be the external forcing factor for the precipitation over the large land area.

From Eq. (1), it is clear that the fraction of the total precipitation that is due to local evaporation and is hence controlled by land surface processes over the region ( $P_m(s)/P$ ) is largest when the value of  $L$  is also large. This means that if the air mass streamtube traverses a long distance and gradually reduces its content of advectively derived moisture along the streamline and instead gains moisture that is locally evaporated

along this path, then the precipitation resulting from that moisture admixture is largely locally derived. Thus, the fraction of precipitation that is recycled and the strength of this mechanism of land surface-atmosphere interaction are more significant over large land areas and inner continental regions.

*c. Parameter uncertainty*

Of all the surface hydrologic fluxes, precipitation is the one most characterized by randomness; this process is especially rich in the high frequencies and may be considered a stochastic process. In the context of the precipitation expression here, the parameters composed in  $\Omega$  are considered to be the source of the randomness. The winds, streamtube characteristics, and other general circulation related features represented by the parameter are taken to be characterized by noise fluctuations around a certain mean value. The variable  $\Omega^{-1}$  is taken to be an uncorrelated white noise process with the expectation  $E[\Omega^{-1}]$  and the variance  $\sigma^2$ .

Upon substituting Eqs. (2), (3), and (11) into the continental hydrologic balance, along with the random process representation for the large-scale forcing  $\Omega^{-1}$ , the following time-differential equation for the soil moisture process is obtained:

$$ds_t = \left[ \frac{P_a}{nZ_r} (1 + E[\Omega^{-1}]s_t^c)(1 - \epsilon s_t^r) - \frac{E_p}{nZ_r} s_t^c \right] dt + \left[ \frac{P_a}{nZ_r} s_t^c (1 - \epsilon s_t^r) \right] \sigma dw_t. \quad (12)$$

Here  $dw_t$  is a  $\mathcal{N}(0, 1)$  white noise and it is the derivative of the unit Wiener process. The governing Ito stochastic differential equation for the continental water balance with atmospheric interaction is rewritten as

$$ds_t = G(s_t)dt + g(s_t)\sigma dw_t, \quad (13a)$$

where

$$G(s_t) = \frac{P_a}{nZ_r} (1 + E[\Omega^{-1}]s_t^c)(1 - \epsilon s_t^r) - \frac{E_p}{nZ_r} s_t^c \quad (13b)$$

and

$$g(s_t) = \frac{P_a}{nZ_r} s_t^c (1 - \epsilon s_t^r) \sigma. \quad (13c)$$

**3. Methodologies for estimating model statistics**

*a. Steady-state probability density function*

The stochastic differential equation (13) describes the soil moisture balance on continental spatial scales and it includes the effects of surface hydrology on the interannual variations in precipitation. The evolution of the soil moisture state in Eq. (13) over a short interval of time  $h$ , that is, the displacement of  $s_t$  from the current state, is given by

$$G(s_t)h + \delta s + \mathcal{O}(h), \quad (14)$$

where  $G(s_t)$  may now be interpreted as the rate at which the soil moisture drifts away from the current state. Thus,  $G(s_t)h$  is the total displacement during the interval  $h$ . The fluctuation  $\delta s$  is due to the presence of noise in the evolution of soil moisture. This perturbation results in a diffusion, and it is characterized by  $E[\delta s] = 0$  and  $\text{var}[\delta s] = \sigma^2 g^2(s_t)h$ . Here  $\sigma^2 g^2(s_t)$  represents the average sensitivity of the soil moisture to noise fluctuations in the neighborhood of the current state of the system. An error on the order of discretization,  $\mathcal{O}(h)$ , is associated with Eq. (14).

As a random Markov process, the drift  $G(s_t)$  and diffusion  $\sigma g(s_t)$  coefficients in Eq. (13) may be written in terms of integrals, over all states, of the product of the distance and the transition probability to the current state (Schuss 1980). For the latter coefficient, the square of the relative distance is used to signify the variability due to the diffusion. Using the Chapman-Kolmogorov equation for continuous Markov processes and these definitions, it may be shown that the evolution of the probability density function for the state  $s_t$  of stochastic differential Eq. (13) is governed by the Fokker-Planck equation

$$\frac{\partial f(s_t, t)}{\partial t} = \frac{\partial}{\partial s} G(s_t)f(s_t, t) + \frac{1}{2} \sigma^2 \frac{\partial^2}{\partial s^2} g^2(s_t)f(s_t) \quad (15)$$

(Schuss 1980).

After a long period, the stationary annual soil moisture stochastic process attains the steady-state probability density function

$$f_{ss}(s) = f(s, t \rightarrow \infty) \quad (16a)$$

when

$$\frac{\partial f(s, t)}{\partial t} = 0. \quad (16b)$$

Equation (15) then becomes an ordinary differential equation whose solution is

$$f_{ss}(s) = C \exp \left\{ -\frac{2}{\sigma^2} U(s) \right\}, \quad (17)$$

where  $C$  is a normalization constant to ensure that Eq. (17) conserves probability mass and integrates to one. The function  $U(s)$  is referred to as the potential

$$U(s) = -\int^s \frac{G(u)}{g^2(u)} du + \sigma^2 \ln g(s). \quad (18)$$

Rodriguez-Iturbe et al. (1991) give the expression for  $f_{ss}(s)$  in the case of the continental water balance model described here.

The useful interpretation of the potential function  $U(s)$  associated with the steady-state probability density function  $f_{ss}(s)$  is that it represents the landscape over which a particle, namely, the current state of the soil

moisture, moves in response to random perturbations. If the probability density function  $f_{ss}(s)$  is Gaussian or unimodal, then the corresponding potential landscape would be a depression with its well located at the statistical mode of  $f_{ss}(s)$ . A particle on this landscape rolls up and down the sides of the well in response to random impulses, but it is ultimately confined to this single well and resides in the well depression most of the time.

### b. Intransitive behavior and multiple equilibria

As evident in the governing evolution Eq. (13), the surface soil moisture balance contains a nonlinear atmospheric feedback term in the form of  $g(s)$  that multiplies the simple white noise random term. Such a multiplicative noise situation may lead to the bifurcation of the potential landscape into a multiplicity of depressions and wells. There will be several new and stable depressions formed that will attract the moving particle. Noise-induced fluctuations will, if strong enough, jolt the particle to escape one depression and fall into the next. Ridges between depressions will be unstable residences for the particle, and the particle will thus spend little time at those locations. Such a landscape will have a multimodal probability density function associated with it. The several modes that arise (the one at the dry end to be called the "drought" and the one at the more moist extremity to be called "pluvial" in the case of soil moisture with a bimodal probability density function) are due to the presence of feedbacks in the water balance equation. Once in a drought (near the drought mode or in the neighborhood of the depression of the potential function at the low soil moisture end), the evaporation rate and hence the local supply of precipitation water diminishes. The drought is reinforced and it persists until a strong enough anomaly in the form of external random noise forcing (i.e., general or large-scale circulation forcing on precipitation) occurs that will be the fluctuation-induced route for escaping drought. Similar arguments apply to the pluvial mode and the local depression in the potential landscape associated with it. It must be noted that standard time series models used in climate and hydrologic time series modeling (e.g., ARMA) are additive noise models, and they are thus restricted to unimodal statistical distributions.

The moving particle on the landscape is agitated by random noise whose intensity or energy level is measured by the variance  $\sigma^2$ . It follows that the stronger the noise (larger  $\sigma^2$ ), the more frequent the jumps will be from one depression (statistical mode) to another. There are, however, a number of other factors involved. The transition time of the particle between modes depends not only on the level of its excitation (i.e.,  $\sigma^2$ ) but on the shape of landscape as well. The deeper the wells and the higher the ridges between these depressions, the more energy it takes to overcome them. Thus, the random fluctuation that results in a successful escape must have a higher magnitude. In terms of the

white noise, this means less probable. Besides the topography of the landscape, the other factor that affects transition time between statistical modes is the multiplicative nature of the noise itself. The position of potential landscape itself is randomly fluctuating in time as the noise multiplies the state variable. The intensity of these landscape fluctuations also depends on the variance of noise  $\sigma^2$ .

The important feature of the water balance model in Eq. (13) is that it represents the governing relation in soil hydrology and that it incorporates land surface-atmosphere interaction in the supply of moisture to regional precipitation. A further important feature is that this model is forced by simple white noise, which represents randomness in the large-scale forcing anomalies for the continental region. Due to the structure of the land surface-atmosphere interaction and the feedback mechanism, the random forcing is multiplicative rather than additive; perturbations may thus develop into persistent anomalies, and the climate may attain a multiple number of preferred modes with noise-induced transitions between the modes.

### c. Estimation of transition times

Here  $\omega$  is defined as the domain of soil moisture  $s_t$  in a drought (or pluvial) mode and  $\omega^c$  is the complement of  $\omega$ , that is, pluvial (or drought) mode. Also we define  $\delta\omega$  as the landscape ridge between  $\omega$  and  $\omega^c$ . Once in  $\omega$ , the first passage out of  $\omega$  to  $\delta\omega$  takes at least an amount of time

$$\tau = \inf\{t \geq u | s_t \in \omega, s_u \in \delta\omega\}. \quad (19)$$

The expected (first moment  $T_1$ ) exit time out of  $\omega$  is

$$T_1 = E[\tau]. \quad (20)$$

(The  $m^{\text{th}}$  moment is  $T_m$ .) Schuss (1980) shows that since  $T_m$  is related to the conditional probability of a transition, then the steady-state  $T_m$  is governed by the analogous Fokker-Planck equation

$$G(s) \frac{dT_m}{ds} + \frac{1}{2} \sigma^2 g^2(s) \frac{d^2 T_m}{ds^2} = -mT_{m-1}. \quad (21)$$

(Here  $T_0 = 1 \forall s$ .) Considering the expected exit time out of  $\omega$  (i.e.,  $T_1$ ), it should be noted that the actual expected transition time out of drought is  $2T_1$ . This is due to the fact that Eq. (21) governs exit time to  $\delta\omega$  on the ridge between  $\omega$  and  $\omega^c$ . At this point, and with equal probability, the Gaussian random fluctuation will take on either sign (positive or negative). And depending on the sign, the evolution of  $s_t$  will either bring it back to  $\omega$  or successfully complete the escape to  $\omega^c$ . Thus, the expected transition time out of a mode associated with the product of probabilities is  $2T_1$ , where  $T_1$  is governed by Eq. (21).

In order to solve this last equation, two boundary conditions are required. One obvious condition is when  $\tau$  in Eq. (21) goes to zero for  $s_t \in \delta\omega$ ;

$$T_m(s_t \in \delta\omega) = 0. \quad (22)$$

This is an absorbing boundary condition indicating that once on the ridge between depressions, the transition to either  $\omega$  or  $\omega^c$  requires almost no time, since points on  $\delta\omega$  are unstable. The second and final boundary condition is to define a reflecting boundary across which  $s_t$  cannot trespass. For the drought mode, this would be the zero limit to the relative soil saturation; at the pluvial mode, the unity upper limit to the relative soil saturation defines this boundary. At these reflecting boundaries, the probability density function itself vanishes. This means that the soil moisture state rarely resides close to this boundary, and escape from its neighborhood is without delay. In this case, the exit time from a region at the reflecting boundary is no different than that from a region a finite distance away from the boundary. This defines a vanishing derivative for the exit-time moment, that is,

$$\frac{dT_m}{ds} = 0 \quad \text{at} \quad s_t = \begin{cases} 1 \\ 0 \end{cases} \quad \text{for} \quad \begin{cases} \text{pluvial} \\ \text{drought} \end{cases} \text{ mode.} \quad (23)$$

When there are two modes to the steady-state probability density function  $f_{ss}(s)$ , then  $\delta\omega$  is taken as the second of the three roots of

$$\frac{\partial U(s)}{\partial s} = 0, \quad (24)$$

where the wells and the ridge are located. These correspond to the statistical modes and the local minimum between them when interpreted in terms of the probability density function  $f_{ss}(s)$ .

With Eqs. (17) and (21), the presence of and persistence in drought and pluvial modes for two case examples, a semiarid and a semihumid climate, will now be analyzed.

#### 4. Climate case examples

The system defined by Eq. (13) will characterize different continental climatic regions depending on the choice of parameters. Here two different climates will be considered in order to illustrate the characteristics embedded in the continental water balance model. The long-term probability distribution function of the soil moisture will be evaluated for each climatic case. Other statistical properties such as the expected duration of persistent dry or wet conditions will be estimated for both climate types.

The two diverse climatic situations that are defined will be referred to as semiarid and semihumid. For both cases,  $L = 2500$  km is taken to be the characteristic length of the tortuous mass-flux stream tube traversing the continental region. The specific humidity-weighted vertically integrated average wind speed of this stream-

line is taken as  $4 \text{ m s}^{-1}$  since the weighting favors the surface boundary layer.

For both climatic cases, the runoff ratio Eq. (2) is assigned  $\epsilon = 1$  and  $r = 6$ ; there is little runoff generated unless the soil is rather moist. For the semiarid case, the coefficient  $c$  in the evaporation efficiency is taken as unity. In the case of the semihumid climatic region,  $c = 1/2$ , signifying the presence of vegetation (see Fig. 3). The semiarid climate is taken to be characterized by relatively shallow soils with a moisture storage capacity of  $nZ_r = 0.5$  m. In the semihumid case example,  $nZ_r = 1.2$  m is given, reminiscent of weathered humid landscapes.

The remaining parameters  $P_a$  and  $E_p$  will be defined as continuous (climatic) rates. Since the seasonal cycle is not considered in this application, the climatic rates for precipitation and potential evaporation correspond to annual mean rates. The soil moisture state variable in the model of Eq. (13) is continuous in time, and it is furthermore stationary. For the semiarid case, a large magnitude value for the unrestricted potential evaporation rate  $E_p$  is estimated;  $E_p = 2.2 \text{ m yr}^{-1}$  in this case. For the semihumid climate, where the actual and the potential rates are closer in value,  $E_p = 1.5 \text{ m yr}^{-1}$ . The precipitation  $P_a$  due to sources outside of the continental region in each case is related to the upwind conditions as well as the static stability of the air mass overlying the region (e.g., subtropical deserts under the descending branch and wetter tropics under the ascending branch of the Hadley cell). For the semiarid case,  $P_a = 0.4 \text{ m yr}^{-1}$ , and the upwind precipitable water depth is  $w = 1$  cm. In the more moist semihumid case,  $P_a = 1.0 \text{ m yr}^{-1}$  and  $w = 4$  cm. Given the definitions of  $L$ ,  $u$ ,  $E_p$ , and  $w$ , the composite parameter  $\Omega$  in Eq. (11) is evaluated to be 0.5 for the semiarid case and 2.7 for the semihumid climate for these average conditions.

The water balance Eq. (13) considers  $\Omega$  to be a mean value of a process with some random variability with a Gaussian marginal distribution. The Gaussian white noise is symmetric around the mean value and has a variance  $\sigma^2$ . Depending on the choice of the parameter  $\sigma$ , the climate cases will not only have different amounts of variability but they will also potentially have different mean conditions and long-term probability distributions due to the strong atmospheric feedback. The criterion for finding physically realistic  $\sigma$  values is taken to be the resulting coefficient of variation on total annual precipitation in each climatic case. With  $\sigma = 2.5$  and 1.0 for the semiarid and semihumid cases, respectively, the resultant coefficients of variation are around 20% for the annual rainfall. This value also corresponds to the rainfall observation in Fig. 1. Model sensitivity to this parameter will be explored by varying  $\sigma$  above and below these nominal values in each case in subsequent analyses.

A summary of the model parameters discussed in this section in the semiarid and semihumid climate cases are listed in Table 1.

TABLE 1. Summary of model parameters for the semiarid and semihumid climatic cases.

Parameters	Units	Semiarid	Semihumid
$c$	[·]	1	0.5
$\epsilon$	[·]	1	1
$r$	[·]	6	6
$nZ_r$	[m]	0.5	1.2
$u$	[ms <sup>-1</sup> ]	4	4
$w$	[m]	0.01	0.04
$L$	[m]	$2.5 \times 10^6$	$2.5 \times 10^6$
$E_p$	[m yr <sup>-1</sup> ]	2.2	1.5
$P_a$	[m yr <sup>-1</sup> ]	0.4	1.0

## 5. Statistics for climate cases

### a. Steady-state distributions and the potential landscape

With no random forcing, the equilibrium soil moisture state will be a constant corresponding to the balance between the long-term hydrologic fluxes. If the model in Eq. (13) had additive instead of multiplicative noise [i.e.  $g(s_t) = \text{constant}$ , in which case the model would be analogous to ARMA time series models or other simple Markov chains], then the marginal distribution of the moisture state would have to be of the same type as the random forcing. For such a variation of the model in Eq. (13), with no interaction and feedbacks, the soil moisture distribution would necessarily have only one mode.

The water balance Eq. (13) has the one unique equilibrium solution in the absence of noise ( $\sigma \rightarrow 0$ ). In the presence of small amounts of white noise forcing, Eq. (13) yields steady-state probability distribution functions for soil moisture that are simply near-Gaussian around the unique equilibrium value of the deterministic case, as illustrated in Fig. 5 for the climatic cases in Table 1. With successively high amounts of variability, the soil moisture state will traverse a wider range of trajectories and may sometimes develop a multiple number of modes indicating prolonged periods of dry or wet conditions (see Fig. 5). Diaz (1983) finds that observed moisture anomalies in the interior of the contiguous United States, where precipitation recycling and the influence of the land surface over climate is significant, also follows a bimodal frequency distribution. The bimodal marginal distribution of the soil moisture state results from the inclusion of the land surface-atmosphere interaction in the water balance model (section 2b). The soil moisture state locks into one mode and exhibits some variability around this condition until a strong enough random perturbation is realized and the system undergoes fluctuation-induced transition into another mode.

The inspection of steady-state probability distribution functions and their corresponding potential landscape will reveal the location and the stability of the preferred modes. Figures 6(a-c) and 7(a-c) represent

these functions for the semiarid and semihumid climate cases of Table 1. In each set of figures, the nominal value of  $\sigma$  (explanation in section 4) and two additional sensitivity cases with  $\sigma$  above and below this value are used to plot, on the same abscissas, the steady-state probability distribution and potential functions.

For the semiarid case in Figs. 6(a-c), two distinct modes are evident, with a strong asymmetry in probability mass distribution. The drought mode at low soil saturations is most frequently visited, but there is evidence of an occasional persistence in a wet or pluvial mode. The probability mass of this pluvial mode seems to increase slightly for higher degrees of variability (i.e.,  $\sigma$ ).

The semihumid case also exhibits two distinct modes but with more comparable probability mass weighting at each mode. With the nominal value of  $\sigma$  for the semihumid case, two modes located at  $s = 0.94$  and  $0.27$  appear (Fig. 7b). With lower variability, both modes approach the deterministic equilibrium value with near-symmetric excursions about it. Figure 7c illustrates the role of higher variability (and larger  $\sigma$ ) on the further separation and clearer identification of these modes.

Substituting the model in Eqs. (13b) and (13c) into the expression for the steady-state probability density function in Eq. (17) reveals that the variance parameter  $\sigma^2$  appears together with the constant soil storage capacity  $nZ_r$  (in the form  $nZ_r/\sigma$ ). Hence, one may increase the variability in the soil moisture process by either increasing the variance in the stochastic forcing (through  $\sigma^2$ ) or decreasing the soil storage capacity ( $nZ_r$ ). With less storage capacity, even small perturbations in precipitation are manifested as large changes in soil moisture. Such a model response and sensitivity are intuitive and are commonly found in many hydrologic modeling applications.

These steady-state probability distribution functions show the relative amount of time the soil moisture state resides at each permissible value; they contain no information on the period of time each mode is continuously occupied nor do they provide clues as to the temporal signature of the stochastic process. The potential functions associated with each probability distribution function in Figs. 6(a-c) and 7(a-c) are, however, indicative of the kind of inducement the system has to go through, in terms of waiting time, for it to escape either mode.

In Figs. 6(a-c) and 7(a-c), the ease with which the soil-moisture state escapes locking into either the drought or the pluvial mode is proportional to the potential height  $\Delta U = U(s_0) - U(s_1)$  it must overcome in order to transition out of a mode. Here  $s_0$  is the soil moisture at the potential landscape ridge between either modes (in  $\delta\omega$  corresponding to a local minimum for the probability density function), and  $s_1$  is the soil moisture for a statistical mode (local peak in the probability density function or either well in the potential landscape). From these figures, it is evident that the

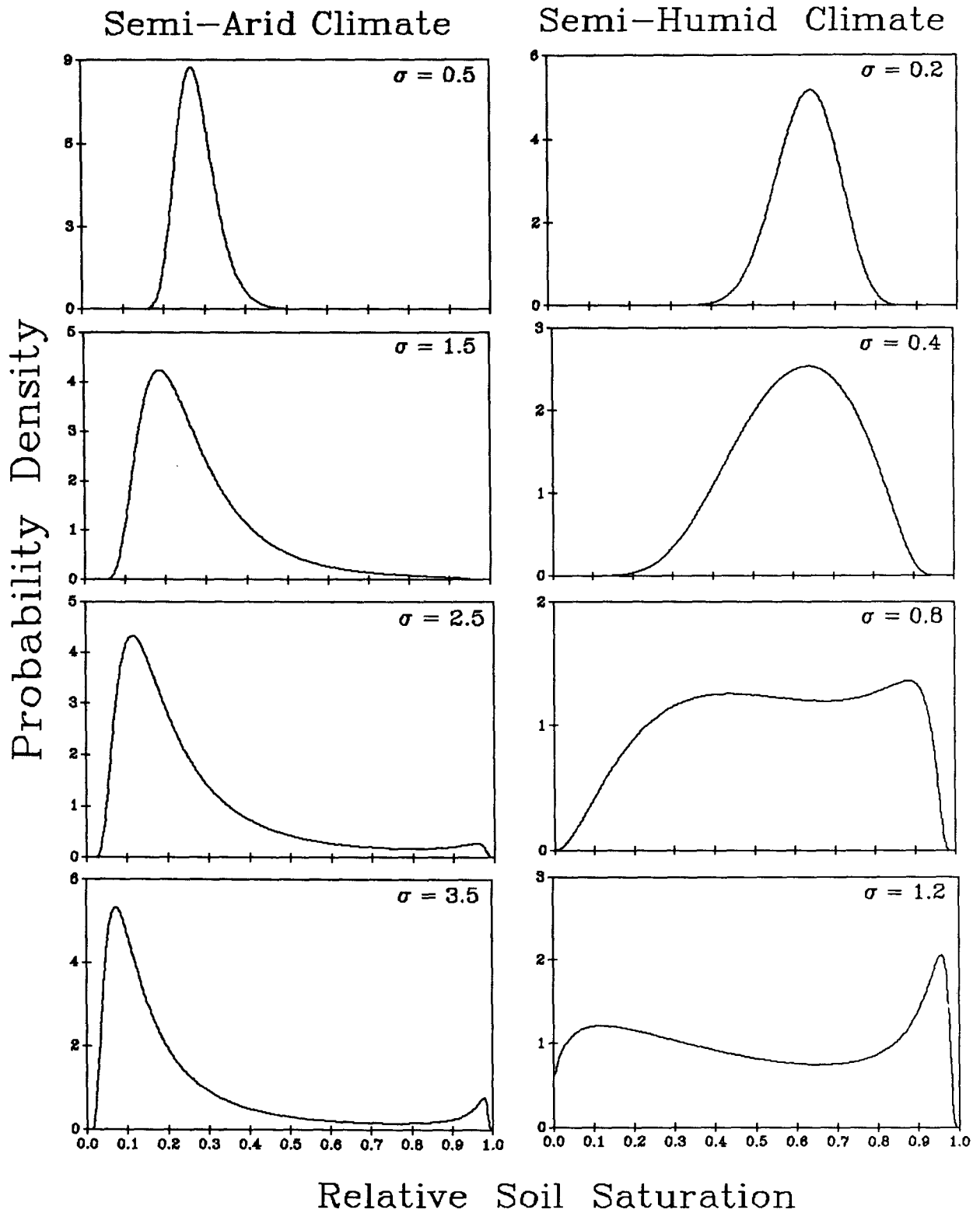


FIG. 5. The steady-state probability distribution function for soil moisture in both climate cases (column 1: semiarid; column 2: semihumid). With low amounts of variance  $\sigma^2$ , the distribution is near-Gaussian around the fixed equilibrium value that would result from the deterministic ( $\sigma = 0$ ) situation. With successively larger amounts of variance, the distribution traverses a larger domain and develops multiple modes in both cases.

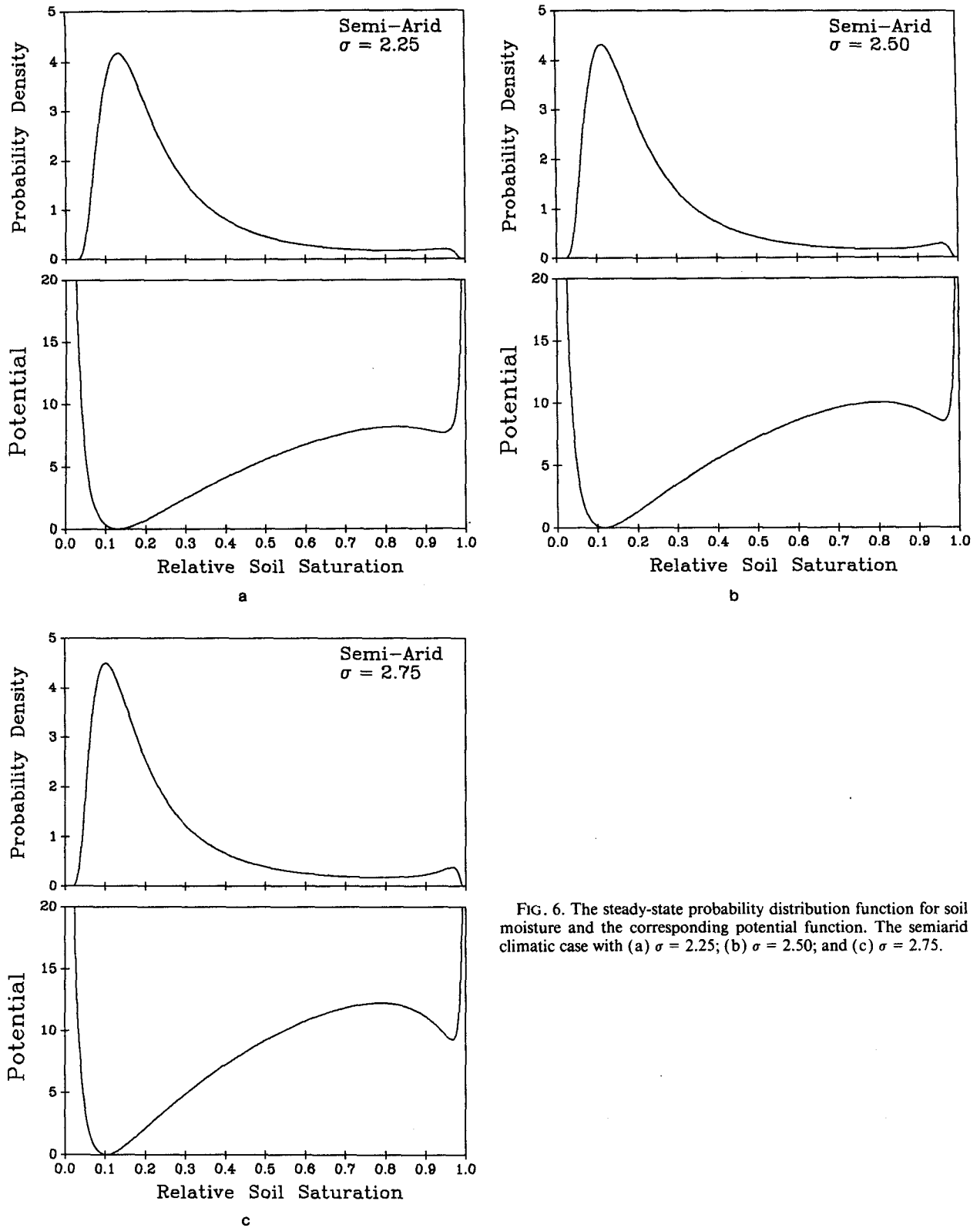
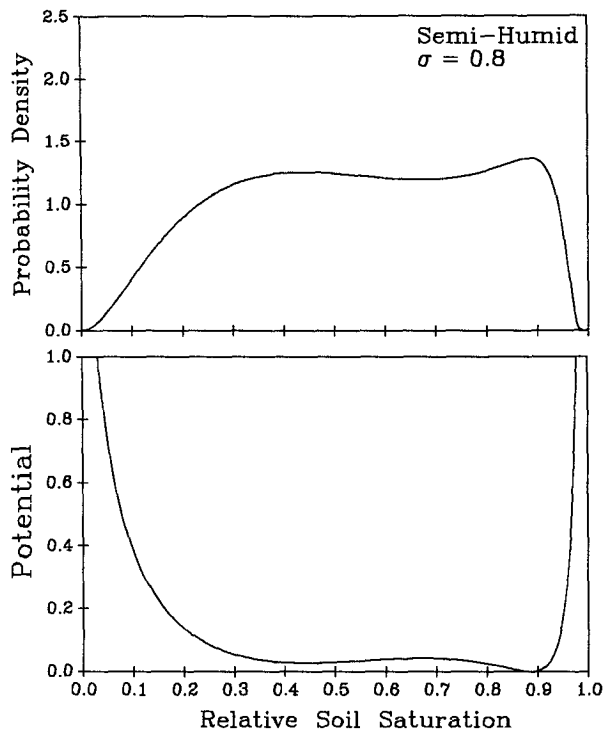
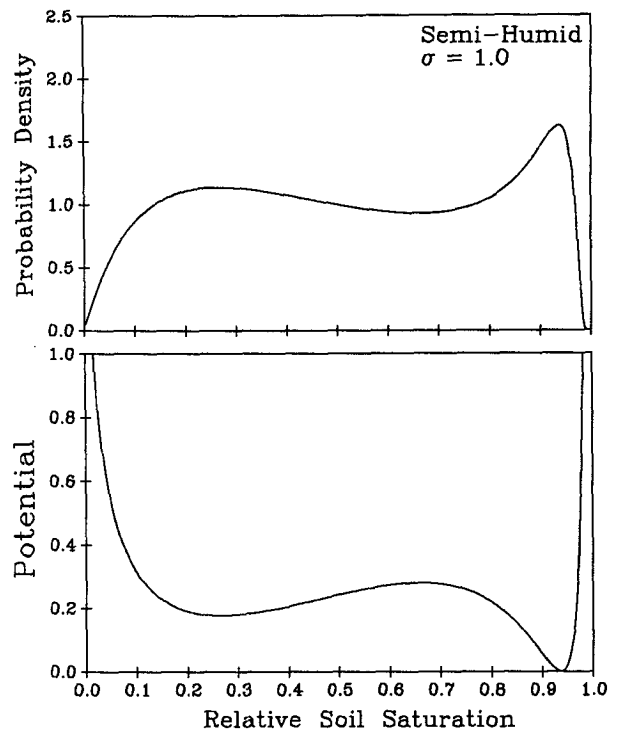


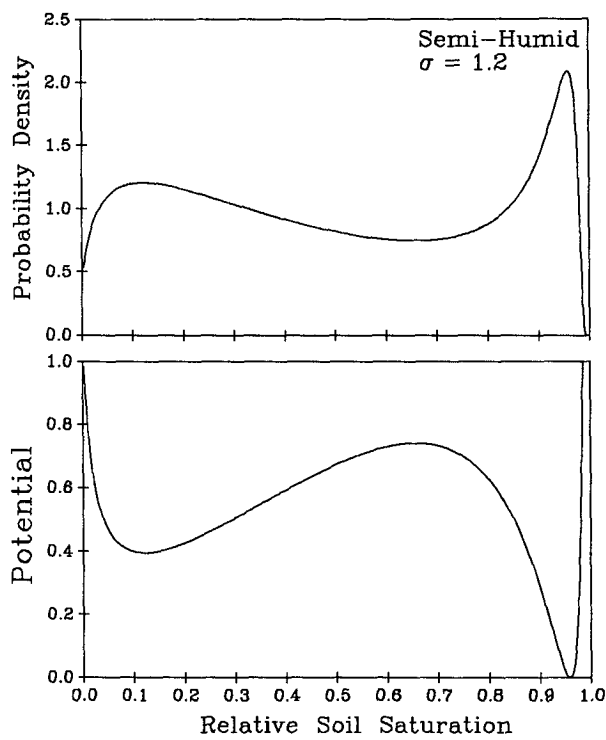
FIG. 6. The steady-state probability distribution function for soil moisture and the corresponding potential function. The semiarid climatic case with (a)  $\sigma = 2.25$ ; (b)  $\sigma = 2.50$ ; and (c)  $\sigma = 2.75$ .



a



b



c

FIG. 7. The steady-state probability distribution function for soil moisture and the corresponding potential function. The semihumid climatic case with (a)  $\sigma = 0.8$ ; (b)  $\sigma = 1.0$ ; and (c)  $\sigma = 1.2$ .

obstacle  $\Delta U$  is higher for the probability density function with the more distinct multiple modes associated with higher values of  $\sigma$ . One would then expect that transition time out of a mode and into another is more prolonged for these cases. There is, however, another contributing factor to consider in regards to transition times. A lower barrier ( $\Delta U$ ) does not ensure more frequent transitions between modes (see the discussion in section 3b). With low amounts of variability, a particle is more sluggish, and even though the barrier to overcome ( $\Delta U$ ) is smaller, the large-magnitude perturbations required for fluctuation-induced transitions are less frequent. The expected transition time may thus be longer than in the case with large amounts of variability in the system. These factors must all be considered in interpreting the moments of transition times estimated using methodologies outlined in section 3c.

#### b. Statistics of transition times between modes

In the water balance Eq. (13) with the bimodal distributions presented in Figs. 6(a-c) and 7(a-c), the soil moisture state persists in one mode and occasionally experiences fluctuation-induced transitions into the other mode; the process is repeated in the reverse direction as well. Since the times elapsed between transitions are themselves random, the overall process is stationary and no spurious periodicities are developed. The probability distribution of these transition times is of interest since it indicates the relative frequency when the water balance equation experiences locking into one mode with interannual persistence in that mode, for example, drought.

In order to characterize the probability distribution function of escape transition times for both the drought and pluvial modes in each climatic case, the first few moments of the distribution function is estimated by solving the governing boundary-value problem of Eqs. (21)–(23). The  $m$ th moment of the transition time  $T_m$  is the conditional value for transition from the current soil moisture to past the potential ridge  $\delta\omega$  and over to the domain of attraction of the next mode.

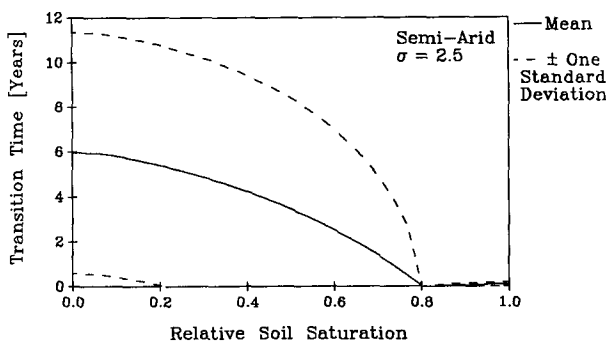


FIG. 8. The mean transition time and one standard deviation brackets for the drought and pluvial models of the semiarid climatic case.

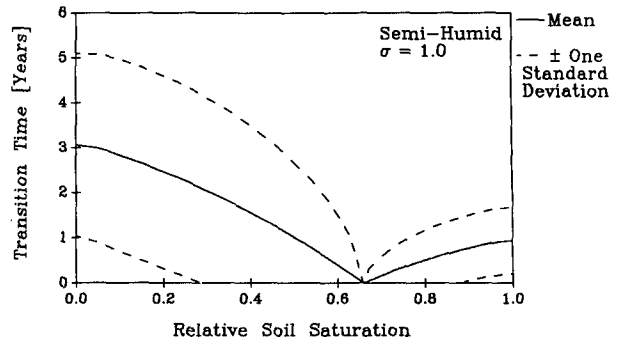


FIG. 9. The mean transition time and one standard deviation brackets for the drought and pluvial modes of the semihumid climatic case.

Thus,  $T_m$  is a function of soil moisture and it vanishes to zero at the unstable point between the two modes [Eq. (22)].

Figures 8 and 9 are plots of the mean transition time with one standard deviation brackets for escape from the drought mode (left-hand side curves) and the pluvial mode (right-hand side curves). The mean and standard deviation are zero at the inflection-point between modes for both the drought and pluvial mode escapes [boundary condition in Eq. (22)]. The slope of  $T_m$  goes to zero at the reflecting boundaries [Eq. (23)]. Figures 8 and 9 use the parameter set defined in Table 1 and section 4 for each climatic case.

In the semiarid climate, the mean escape time from drought may be up to 6 years; there is considerable variability about this mean as indicated by the wide region covered by the one standard deviation brackets around the mean value in Fig. 8. Persistence and locking into the drought mode is therefore considerable for this climatic case. There is nevertheless occasional transitions into wetter or pluvial conditions. There is little persistence in this mode, as indicated by the small mean transition time in Fig. 8 and the relatively low amount of probability mass under the pluvial mode in the distributions (Fig. 6b).

The semihumid case has a mean transition time of up to 3 years for escaping drought and less than 1 year for escaping pluvial modes (Fig. 9). There is, as in the semiarid case, considerable variability around this mean value as indicated by the wide bracket for the standard deviation below and above the mean in Fig. 9. In fact, as evident in the crossing of the standard deviation curve into the abscissa in Figs. 5 and 6, the probability distribution of transition times has a strong positive skew. Plots of the cube-root third central moment for escape time from the drought and the pluvial modes appear in Fig. 10 for the semiarid case and Fig. 11 for the semihumid case.

The statistical moments for the transition times between drought and pluvial modes for each climatic case indicate that the period of time the water balance interannual variability persists in one moisture condition

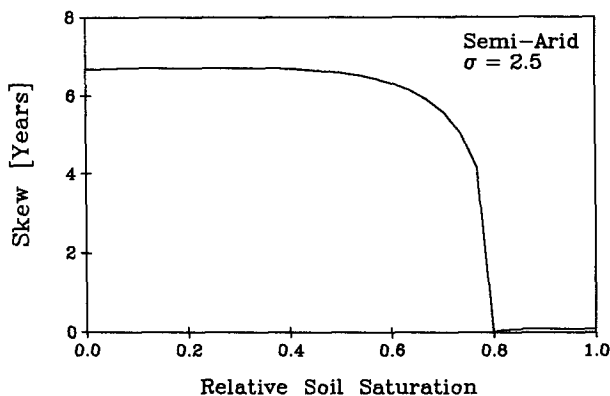


FIG. 10. The skew of the transition time out of the drought and pluvial modes of the semiarid climatic case.

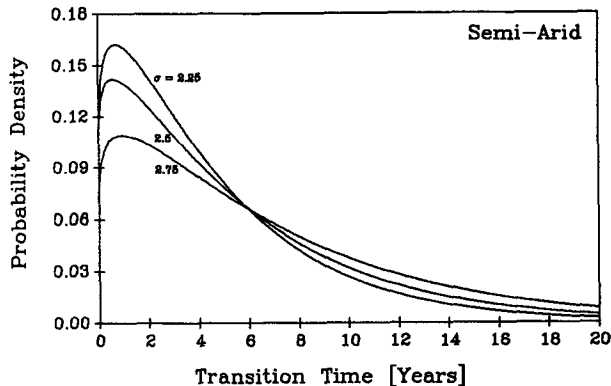


FIG. 12. The approximate probability distribution functions of transition times from under the drought mode for the semiarid climatic case.

is generally brief. But occasionally and with considerable probability, the climate persists in drought for some years—up to a decade or more. This characteristic is brought about by the strong land-surface-atmosphere interaction in supplying the precipitation of large continental regions.

Based on the first three moments in Figs. 8–11, the approximate probability distribution function of transition times is found from under the drought mode. Figures 12 and 13 illustrate these distributions for the semiarid and semihumid climatic cases; the three curves in each figure correspond to the different values for variance  $\sigma^2$  used in Figs. 6(a–c) and 7(a–c). These distributions are approximated using a method-of-moments parameter estimation for a Beta- $P$  function, with three parameters or degrees of freedom constrained to reproduce the first three moments (Selker and Haith 1990).

The probability distribution of escape times out of the drought mode for the semiarid climate has a preference for shorter periods (Fig. 12). But there is considerable probability mass remaining for much longer periods of up to two decades. Droughts of this long

duration are occasionally realized and the curves in Fig. 12 indicate that this characteristic more so applies to high  $\sigma^2$  cases.

Figure 13 represents the approximate transition-time probability distributions for the semihumid case with  $\sigma = 0.8, 1.0,$  and  $1.2$ . The short transitions and escapes from under the drought are more frequent than longer duration ones. Nevertheless and with considerable probability, the drought may persist for up to 5–6 years in the semihumid climatic case.

*c. Simulations*

In order to inspect the bimodal characteristic of the intransitive climates presented here and to illustrate the random nature of the interannual persistence periods of anomalies, the water balance equation for each climatic case is integrated. Because of the stochastic calculus in Eq. (13), standard numerical integration techniques do not apply. The methodology presented by Milshtein (1974) is used to integrate the stochastic differential equation.

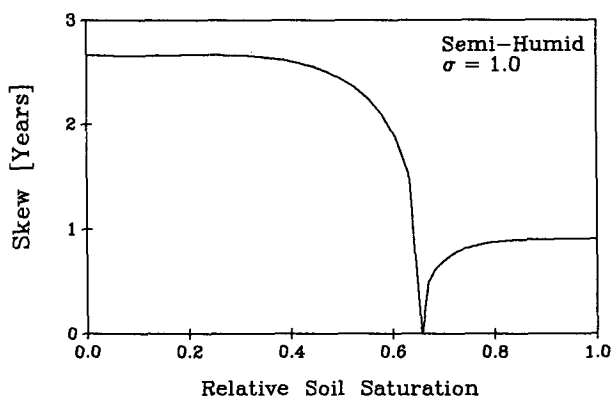


FIG. 11. The skew of the transition time out of the drought and pluvial modes of the semihumid climatic case.

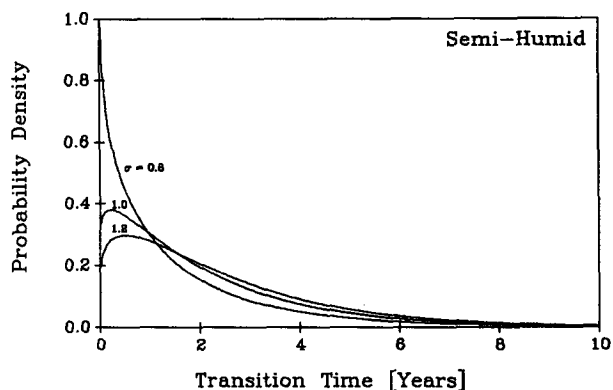


FIG. 13. The approximate probability distribution functions of transition times from under the drought mode for the semihumid climatic case.

Figures 14 and 15 show the accuracy of the simulation technique in reproducing the theoretical steady-state probability distribution function; the bimodal characteristic for both the semiarid and semihumid climatic cases is also evident in the simulation frequency distribution. The time series realizations for each climatic case (Figs. 16a, b) illustrate the bimodality as well as the transition-time characteristics. In the semiarid case in Fig. 16a, the soil moisture state is predominantly dry with occasional excursions into moist anomalous conditions. While dry periods last on the order of one decade, more moist periods govern for only a few years or less. The semihumid climatic case (Fig. 16b) has similar drought and pluvial modes with occasional transitions between the two. In both modes, the condition may persist for up to several years.

The precipitation associated with the stochastic differential equation for continental water balance may be determined through the numerical integration of Eqs. (11) and (13) based on when equations are posed in differential form. This precipitation process includes both the large-scale advective and the locally supplied (through evapotranspiration) sources of moisture. Figure 17a illustrates the statistical frequency distribution for the precipitation in the case of the semiarid climate. Similarly, Fig. 17b contains the distribution for the semihumid case. They are both characterized by bimodal distributions due to the influence of the regional soil hydrology on the precipitation.

## 6. Conclusions

The governing hydrologic balance for the soil water store in large land areas is defined and it is coupled with a model of land surface-atmosphere interaction. In the model, precipitation over the land surface region is derived from atmospheric moisture that is supplied by both external advection over to the land region and evapotranspiration from within the boundaries of the land area. Since the soil hydrology controls the rate of evapotranspiration, an interaction between the land

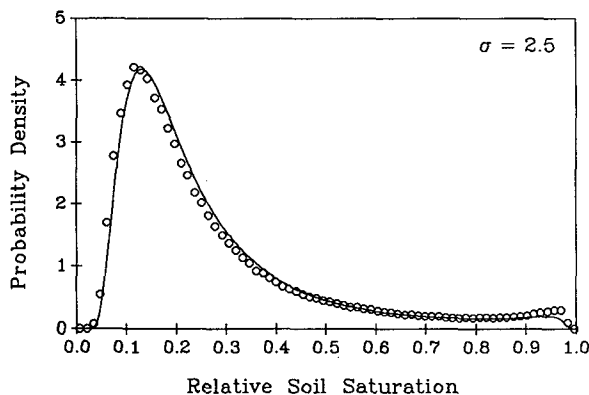


FIG. 14. The theoretical (solid line) and the simulated (symbols) probability density function for soil moisture in the semiarid case.

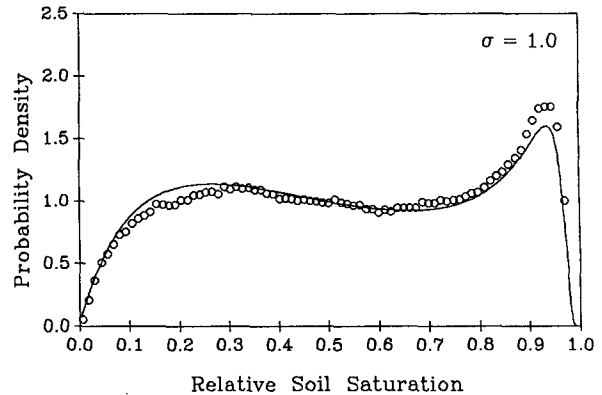


FIG. 15. The theoretical (solid line) and simulated (symbols) probability density function for soil moisture in the semihumid case.

surface and the atmosphere develops, whereby the precipitation rate is partially controlled by the state of soil moisture that is itself a result of the precipitation regime. When the regional climate is externally forced by simple random perturbations (white noise in this model), the soil moisture state nevertheless attains a bimodal frequency distribution. The resulting intransitive climate persists in one mode and occasionally transitions to the other mode only in the presence of strong noise inducements. The result is a model of large-scale hydrology, whereby persistent droughts are found to result from the routing of simple noise through a web of interactions and feedbacks in the land-atmosphere system.

The statistical moments characterizing the probability distribution of transition times between the distinct modes of climates are estimated for two cases. It is shown that droughts may persist for up to several years in semiarid and semihumid continental climates due to land-surface feedbacks.

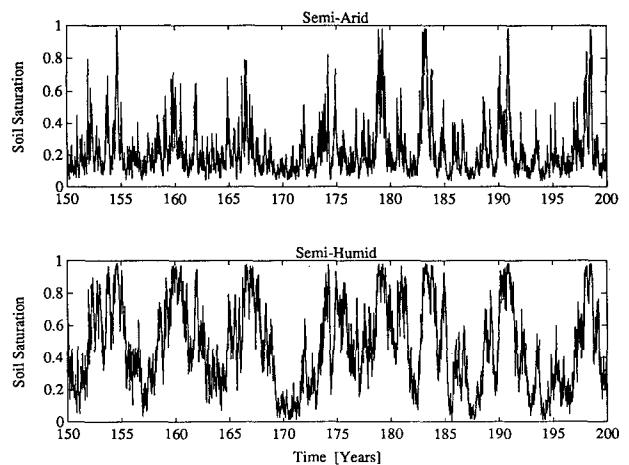


FIG. 16. Simulated time series of soil moisture using Eq. (13) for the (a) semiarid and (b) semihumid climatic cases.

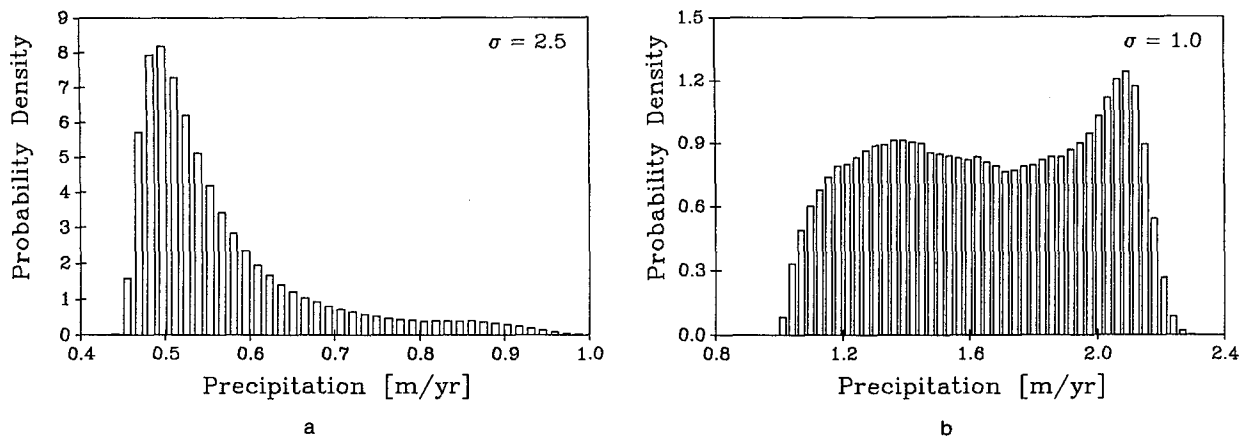


FIG. 17. The simulated probability density function for the total precipitation (in  $\text{m yr}^{-1}$ ) in the (a) semiarid and (b) semihumid cases.

These consequences of the land surface partial control over the precipitation regime in continental-type climates illustrates the importance of surface hydrology for the dynamics of large-scale climates. The modeling of global climate and the statistical characterization of significant climatic interannual variability must incorporate the role of land surface hydrology and take into account not only moisture supply but other ways in which surface conditions force the larger-scale atmosphere.

**Acknowledgments.** Support for this work has been provided, in parts, by National Science Foundation Grants EAR-9120367, EAR-9120386, and BCS-9158150. The research leading to this paper took place while D. Entekhabi was at the Department of Hydrology and Water Resources at The University of Arizona and Ignacio Rodriguez-Iturbe was at the Iowa Institute of Hydraulic Research at The University of Iowa. The support of The University of Arizona School of Engineering and the Iowa Economic Development Commission is gratefully acknowledged.

#### REFERENCES

- Brubaker, K. L., D. Entekhabi, and P. S. Eagleson, 1991: Atmospheric water vapor transport: Estimation of continental precipitation recycling and parameterization of a simple climate model. MIT Department of Civil Engineering, Ralph M. Parsons Laboratory Report No. 333, 166 pp.
- Budyko, M. I., 1974: *Climate and Life*. Academic Press, 508 pp.
- Chagnon, S., 1987: Detecting drought conditions in Illinois. *ISWA/CIR-169-87*, 36 pp.
- Charney, J. G., P. H. Stone, and W. J. Quirk, 1975: Drought in the Sahara: A biogeophysical feedback mechanism. *Science*, **187**, 434–435.
- Diaz, H. F., 1983: Some aspects of major dry and wet periods in the contiguous United States, 1895–1981. *J. Climate Appl. Meteor.*, **22**, 3–16.
- Eagleson, P. S., 1982: *Land Processes in Atmospheric General Circulation Models*. Cambridge University Press, 560 pp.
- Eltahir, E. A. B., 1989: A feedback mechanism in the annual rainfall, Central Sudan. *J. Hydrol.*, **110**, 323–334.
- Hare, F. K., 1985: *Climate Variations, Drought and Desertification*. WMO, No. 653, 35 pp.
- Idso, S., R. Jackson, R. Kimball, and F. Nakayama, 1975: The dependence of bare soil albedo on soil water content. *J. Appl. Meteor.*, **14**, 109–113.
- Karl, T. R., 1983: Some spatial characteristics of drought duration in the United States. *J. Climate Appl. Meteor.*, **22**, 1356–1366.
- , F. Quinlan, and D. S. Ezell, 1987: Drought termination and amelioration: Its climatological probability. *J. Climate Appl. Meteor.*, **26**, 1198–1209.
- Koster, R., J. Jouzel, R. Souzzo, G. Russel, D. Rind, and P. S. Eagleson, 1986: Global sources of local precipitation as determined by NASA/GISS GCM. *Geophys. Res. Lett.*, **13**(1), 121–124.
- Lettau, H., K. Lettau, and L. C. Molion, 1979: Amazonia's hydrologic cycle and the role of atmospheric recycling in assessing deformation effects. *Mon. Wea. Rev.*, **107**, 227–238.
- Lowry, W. P., 1959: The falling rate phase of evaporative soil moisture loss: A critical evaluation. *Bull. Amer. Meteor. Soc.*, **40**, 605.
- McDonald, J., 1962: The evaporation–precipitation fallacy. *Weather*, **17**, 168–177.
- McNab, A. L., 1989: Climate and drought. *EOS*, American Geophysical Union, **70**(40), 873.
- Milshstein, G. N., 1974: Approximate integration of stochastic differential equations. *SIAM Theory of Probability and Its Applications*, **19**(3), 557–562.
- Namias, J., 1983: Some causes of United States drought. *J. Climate Appl. Meteor.*, **22**(1), 30–39.
- Nicholson, S. E., and D. Entekhabi, 1986: The quasi-periodic behavior of rainfall variability in Africa and its relationship to the Southern Oscillation. *Arch. Meteor. Geophys. Biophys., Series A*, **34**, 311–348.
- Rodriguez-Iturbe, I., D. Entekhabi, and R. L. Bras, 1991: Nonlinear dynamics of soil moisture at climate scales: 1. Stochastic analysis. *Water Resour. Res.*, **27**(8), 1899–1906.
- Rowntree, P. R., and J. A. Bolton, 1983: Simulations of the atmospheric response to soil moisture anomalies over Europe. *Quart. J. Roy. Meteor. Soc.*, **109**, 501–526.
- Schuss, Z., 1980: *Theory and Applications of Stochastic Differential Equations*. John Wiley and Sons, 321 pp.
- Selker, J. S., and D. A. Haith, 1990: Development and testing of single-parameter precipitation distributions. *Water Resour. Res.*, **26**(11), 2733–2740.
- Stidd, C. K., 1975: Irrigation increases rainfall? *Science*, **188**, 279–280.
- Voice, M. E., and B. G. Hunt, 1984: A study of the dynamics of drought initiation using a global general circulation model. *J. Geophys. Res.*, **89**(D6), 9504–9520.
- Yeh, T. C., R. T. Wetherald, and S. Manabe, 1984: The effect of soil moisture on the short-term climate and hydrology change—a numerical experiment. *Mon. Wea. Rev.*, **112**, 474–490.